Global Journal of Engineering and Technology Advances

eISSN: 2582-5003

Cross Ref DOI: 10.30574/gjeta

Journal homepage: https://gjeta.com/

(Research Article)

Analysis of torque ripples and switching losses of a diode clamped inverter fed permanent magnet synchronous motor drive

P Vinod Kumar [1,*], S Venkateshwarlu [1] and SS Tulasi Ram [2]

[1] *Department of EEE, CVR College of Engineering, Hyderabad, India.*

[2] *Department of EEE, G. Narayanamma Institute of Technology & Science, Hyderabad, India.*

Global Journal of Engineering and Technology Advances, 2022, 11(03), 059–066

Publication history: Received on 14 May 2022; revised on 18 June 2022; accepted on 20 June 2022

Article DOI: https://doi.org/10.30574/gjeta.2022.11.3.0096

Abstract

The modern-day electric vehicles use brush less DC motors (BLDC) and Permanent Magnet Synchronous Motors (PMSM) as the main driving units. The traction systems also have tried PMSM machine as the driving unit. The variable frequency power source is required to control the speed and torque of the motor to meet the load requirements. The Inverter – power modulator is causing the production of ripples in source current and flux components, hence the torque. This paper presents the effect of inverter on the flux and torque ripples. Also, the simulation results of inverter switching losses are discussed.

Keywords: Permanent Magnet Synchronous Motor (PMSM); Diode-Clamped Multilevel Inverter (DCMLI); Switching Losses; Total Harmonic Distortion (THD)

1. Introduction

The multilevel inverters demand is increasing in medium and high-power applications. The main characteristic of multilevel inverters is quality of the voltage or current waveform. This can be implemented with different voltage sources connected in series resulting a high voltage. Power electronics market is expanding its application of multilevel inverter in both power electronics and power systems areas. Variable frequency drives such as Induction motor and synchronous motor drives are mostly using multilevel inverters. The direct supply operation produces a smooth airgap flux and smooth torque. Whereas the inverter fed motors produce a ripple in airgap flux and hence in the electromagnetic torque. These ripples in electromagnetic torque causes humming in motor operation, vibration in mechanical parts and causing a trouble in achieving precise position control.

There are many methods available in literature to minimize the torque ripples. To suppress pulsating torques in PMSMs the instantaneous torque estimation using a rigorous analytical model are considered, which can take into account the spatial harmonics that cause the pulsating torques. To suppress the pulsating torque, the rigorous analytical model and a simplified version have been applied to the generation of the current command for smoothing the torque. The current command is derived by employing both torque FF and FB control. The effectiveness of the torque control has been verified via PMSM and Syn-RM simulations, showing that the superimposed current command obtained from the torque FF and FB control could effectively reduce the torque ripples [1]. According to the periodic characteristics of torque ripple, a method called ILC together with speed control and torque control to reduce the torque ripple of PMSM. The ILC can effectively reduce torque ripple of PMSM. It provides a reference and basis for the PMSM control system design and implementation [2]. Another has proposed a PSC algorithm for 2L-VSIPMSM drive system. The proposed algorithm incorporates DVVs and corresponding SSs into the control set of PSC and utilizes cost function to evaluate the torque and flux ripples while applying different DVVs and SSs. The selected optimal DVV and SS achieves better performance

* Corresponding author: P Vinod Kumar
Department of EEE, CVR College of Engineering, Hyderabad, India.

of torque and stator flux [3]. The application of optimized state selector DTC in permanent magnet synchronous motor drivers is considered. This new method has the same advantage of compact structure of conventional DTC, but results of simulation show that it is super than conventional DTC in the aspects of decrease of fluctuation of flux linkage and electromagnetic torque, robustness of velocity, as well as decrease of switching power wastage of power devices and so on [4].

A simple yet effective duty ratio determination has been presented for duty-based DTC scheme. The steady-state performance and dynamic response performance have been analytically compared to the classic DTC and two previous improved DTC methods. The simulation results confirm that the proposed method achieves lowest torque ripple while not deteriorating the inherent fast transient response performance of the classical DTC. In addition, the parameter sensitivity has been also studied and the results show that the proposed duty-ratio determination method is parameter independent. Featuring simple structure and low computational burden, the proposed DTC is easy to be implemented in practical industrial drive system [5]. A feedback linearization control system for PMSM based on traditional DTC is designed to complete the tracking control of motor torque and flux linkage. Firstly, the torque and flux estimation in the d − q coordinate are completed, which solves the problem of flux-torque mutual coupling in the traditional DTC. Secondly, the Lyapunov theory is applied to let the tracking error of the system satisfy the asymptotic stability condition and get the control rates of ud and uq. Then, the theory of feedback linearization and state feedback is used to complete the design of the system controller. Finally, the system simulation experiments in MATLAB/Simulink environment verify the effectiveness of this scheme. The simulation results show that the feedback linearization control scheme proposed in this paper has better inhibitory effect on the torque and flux ripple of the motor [6].

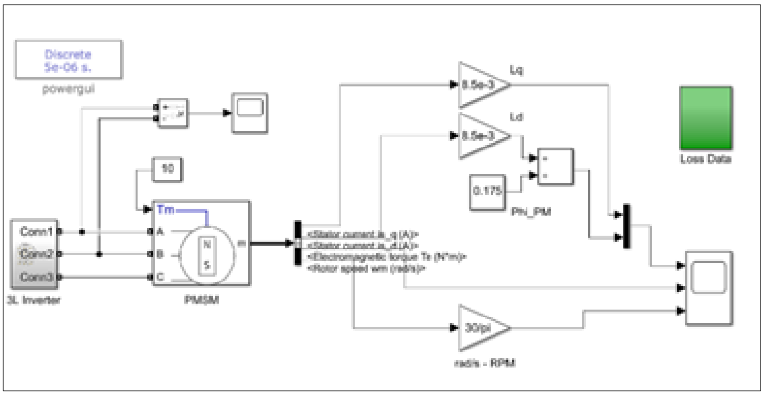

Figure 1 DCMLI fed PMSM – simulink model

2. Diode-Clamped Inverters

For every leg of the three-phase inverter 8 switches are connected. A voltage divider made using 4 capacitors has been incorporated in the circuit to divide the voltage and transform inverter as a five level in the output. Due to heat and power losses capacitor's reactance is chosen over resistor's resistance as voltage divider. The four separate DC sources are placed in such a way that it resembles the topology that of a cascaded H bridge. Each leg contains clamping diodes, this is specifically done to gain control over the input voltage and to protect the switches from the transient voltages. Each device that consists of two switches and a clamping diode has a potential difference V. There are 4 devices across a leg and therefore the total voltage across the leg is 4 times V.

Table 1 Switching table of five level DCMLI

Output Voltage (V_{an})	Sa_1	Sa_2	Sa_3	Sa_4	Sa_5	Sa_6	Sa_7	Sa_8
2V	1	1	1	1	0	0	0	0
V	0	1	1	1	1	0	0	0
0	0	0	1	1	1	1	0	0
-V	0	0	0	1	1	1	1	0
-2V	0	0	0	0	1	1	1	1

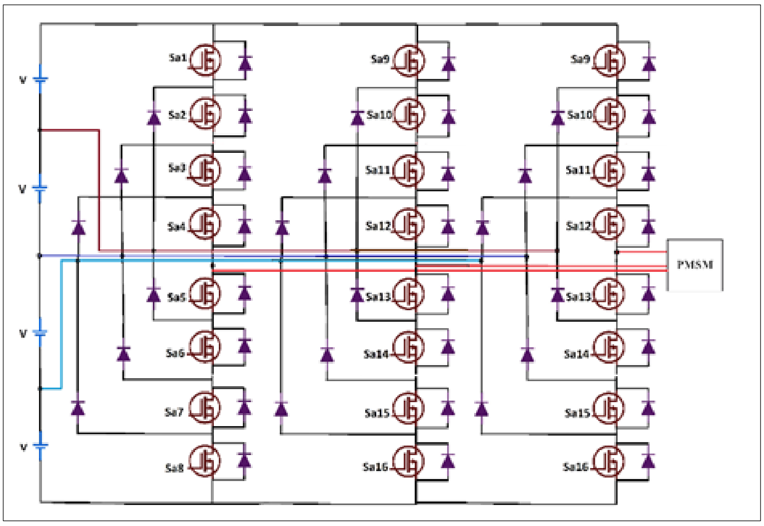

Figure 2 Five-levelDCMLI fed PMSM drive

3. Mathematical model of PMSM

The operation of a PMSM is like a three-phase induction motor. The three-phase voltage source connected with the stator winding produces a rotating magnetic field (RMF). The RMF cause the rotor to turn. The power losses in the rotor side do not occur because the rotor of PMSM is a permanent magnet. Moreover, this machine can provide a constant torque. The structure and equivalent circuit of the PMSM are shown in Fig. 1

The DQ modeling method is applied to derive a mathematical model of the system as depicted in Fig. 2. The DQ– axis in Fig. 3 is rotated with the angular speed (ωr) by phase shift (θr). The stator voltages (Vabc) can be written for three phase system as follows:

$$V_d = R_s i_d + \frac{d}{dt}\psi_d - \omega_r \omega_q$$
$$V_q = R_s i_q + \frac{d}{dt}\psi_q + \omega_r \omega_d$$
$$\psi_d = R_s i_q + \psi_{pm}$$
$$\psi_q = L_q i_q$$

$$V_d = R_s i_d + \frac{d}{dt}(L_d i_d + \psi_{PM}) - \omega_r L_q i_q$$
$$V_d = R_s i_d + L_d \frac{di_d}{dt} - \omega_r L_q i_q$$
$$\frac{di_d}{dt} = \frac{i}{L_d}(V_d - R_s i_d + \omega_r L_q i_q)$$
$$V_q = R_s i_q + \frac{d}{dt}(L_q i_q) + \omega_r (L_d i_d + \psi_{pm})$$
$$V_q = R_s i_q + L_q \frac{di_q}{dt} + \omega_r L_d i_d + \omega_r \psi_{pm}$$

$$\frac{di_q}{dt} = \frac{1}{L_q}(V_q - R_s i_q - \omega_r L_d i_d - \omega_r \psi_{pm})$$

$$T = \frac{3}{2} P[(L_d - L_q) i_d i_q + \psi_{pm} i_q]$$

4. Conduction & switching loss calculation

As switching frequencies increase in the IGBT, *switching losses* occur. These are the losses associated with the transition of the switch from its on-state to off-state, and back. The higher the switching frequency, the greater the number of times the switch changes state per second. By switching the IGBT, either the voltage across the IGBT is close to zero, or the current through it is close to zero, and therefore the dissipation cross-product is also almost zero. The conduction loss is not frequency dependent. It depends on the *duty cycle.*

Conduction losses occur in the switches and the anti-parallel diodes. Conduction loss in the switches can be calculated using equation (1), and conduction loss in anti-parallel diodes can be calculated using equation (2).

$$W_{cs} = U_{CEo} * I_{Cav} + r_c * I_{Crms}^2 \quad (1)$$

$$W_{cd} = U_{Do} * I_{Dav} + r_D * I_{Drms}^2 \quad (2)$$

where

U_{CE0} : On state zero current collector emitter voltage

I_{Cav} : Average switch current

R_c : Collector emitter on state resistance

I_{Crms} : RMS switch current

U_{D0} : Diode approximation with a series conduction of DC voltage sources

I_{Dav} : average diode current

r_D : Diode on-state resistance

I_{Drms} : RMS diode current

Switching losses will be occurred in the switches and the anti-parallel diodes. The switching losses in the switch can be calculated using equation 3. And the switching losses in the anti-parallel diodes can be calculated using equation 4.

$$W_{SwS} = \left(E_{onSw} + E_{offsw}\right) * f_{sw} \quad (3)$$

$$W_{SwD} = \left(E_{onD} + E_{offD}\right) * f_{sw} \approx E_{onD} * f_{sw} \quad (4)$$

where

E_{onSw} : turn - on energy losses in Switch

E_{offsw} : turn - off energy losses in Switch

E_{onD} : turn - on energy losses in diode

E_{offD} : turn - off energy losses in diode

F_{sw} : Switching frequency

5. Results and discussion

In this paper, analysis of conduction loss & switching loss is done for nine-level five-level diode-clamped inverter. To simulate the switching losses, a modified half bridge module is taken from Simulink. Thermal model of IGBT-diode and a simscape based heatsink are considered for switching loss analysis [7]. IGBT module no: GD75HFY120C1S is considered for half bridge module [8]. The thermal model of IGBT-diode is shown in figure 4. The thermal capacitance of the switch and switch to heatsink resistance are also included in the simulation. The heatsink simscape model is shown in the figure 5. The turn on loss is calculated using voltage before switching and current after switching along with the temperature at junction. The turn off loss is calculated using the current before switching and the voltage after switching along with junction temperature. Conduction losses are calculated using the saturation voltage across collector and emitter multiplied with collector current. This process of simulation of losses has done based on the lookup table taken from the MATLAB sources [7].

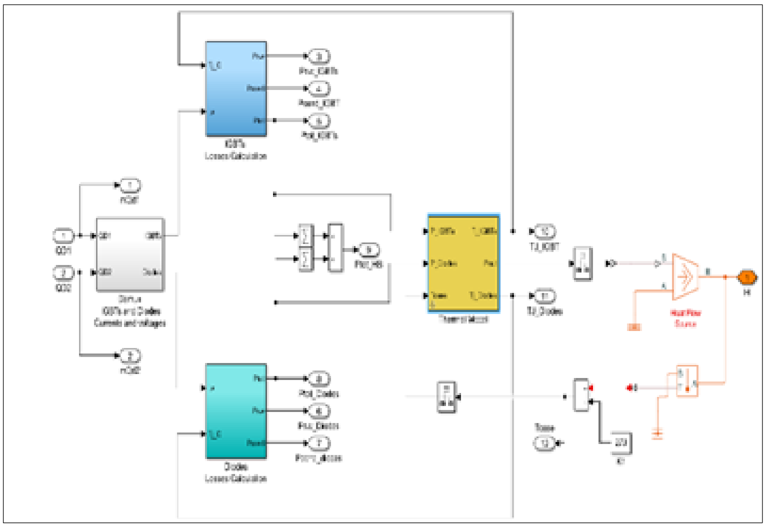

Figure 3 Thermel model of half bridge with IGBTs and diodes

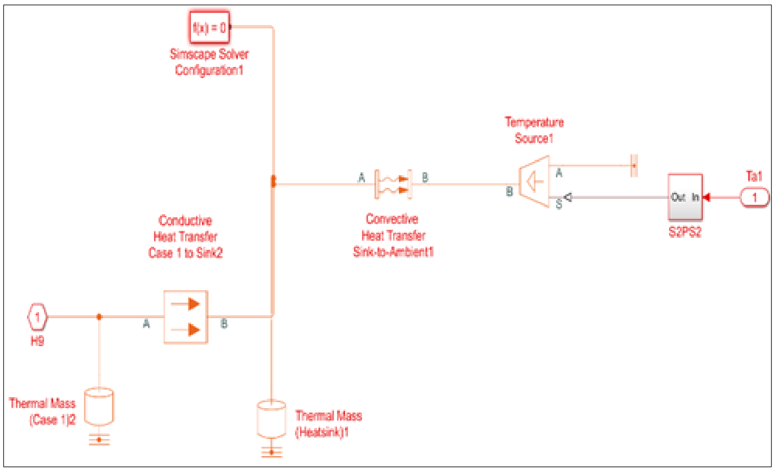

Figure 4 Simscape model of heatsink for half bridge (Two IGBTs)

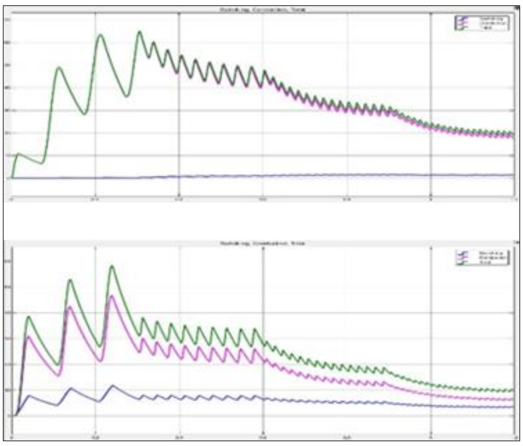

Figure 5 Switching losses of Sa1 and Sa4 of 5 level DCMLI

The switches Sa1 and Sa4 in the figure 2 will have distinctive operation subjected to the period of conduction. Sa1 operates for short period but produces the peak voltage in the output. Sa4 operates for longer periods but produces ¼ th of the peak value. So, these switches are considered for the comparison of switching loss.

Figure 5 shows the total switching losses of the switches Sa1 and Sa4. Switching losses in Sa1 is around 10W and in case of Sa4, it is around 2W. For Sa4, The total switch loss will be conducting loss and the switching loss is negligible.

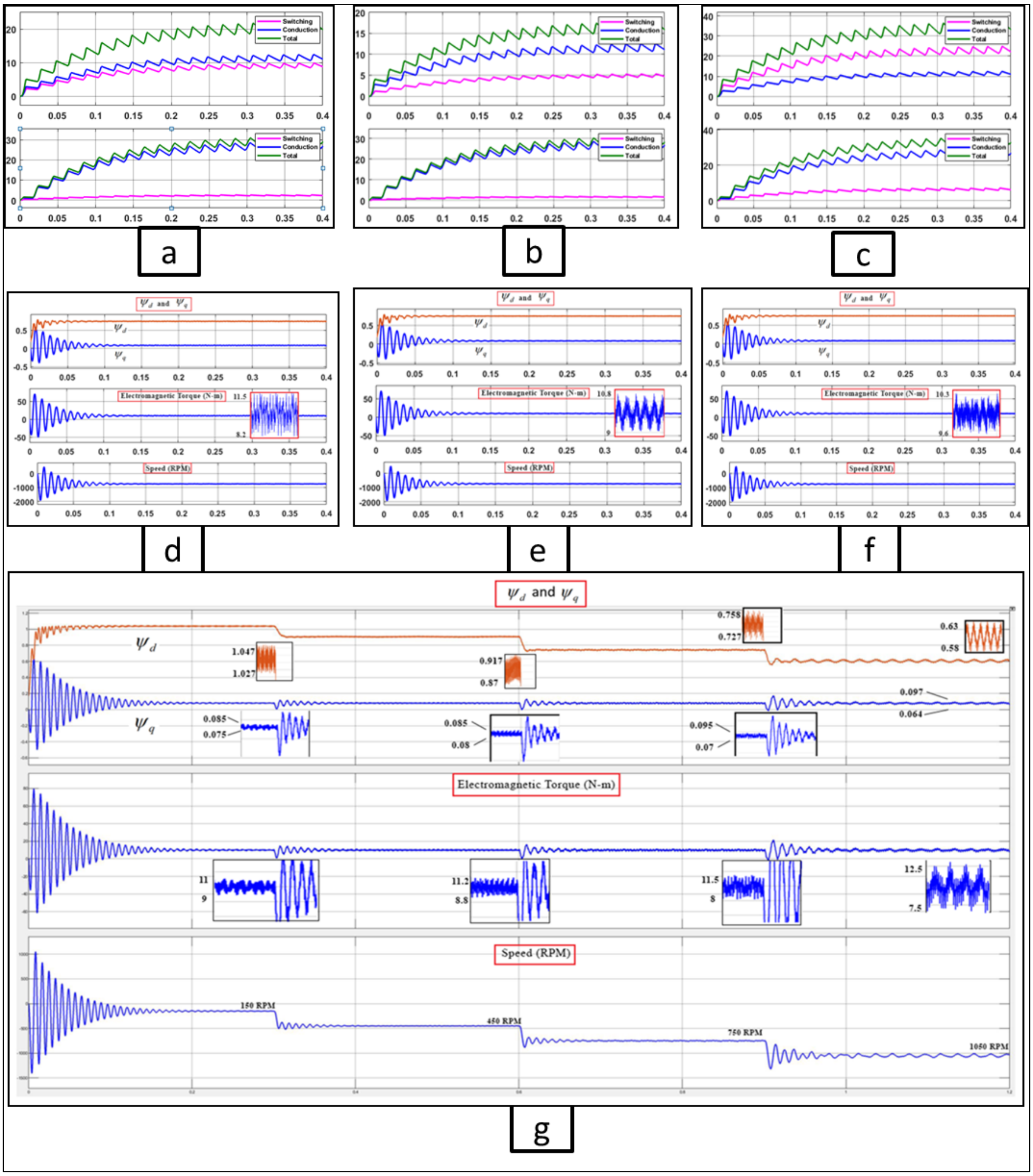

Figure 6 Switching losses of top and Bottom IGBTs simulated for (a) 1000 Hz (b) 2000 Hz (c) 5000 Hz; ψ_d and ψ_q, Electromagnetic torque and speed of PMSM simulated for (a) 1000 Hz (b) 2000 Hz (c) 5000 Hz; (g) ψ_d and ψ_q, Electromagnetic torque and speed of PMSM simulated for 1000Hz switching frequency and four different sine frequencies (150 rpm, 450 rpm, 750 rpm and 1050 rpm)

5.1. For the switch Sa1

In the case of 1000Hz conduction loss and switching losses are equal. Both the magnitudes rise from 0 to 10. The resultant losses are therefore 20W. As both losses are equal the difference between them is zero. In the case of 2000Hz switching losses has a magnitude of 5 and conduction loss has a magnitude of 10. The resultant losses is therefore 15.The difference between conduction loss and switching loss is 5 and conduction loss is greater than switching loss. The variation of the switching loss from the previous case is due to the increase in frequency. The magnitude of the conduction losses remains constant as the duty cycle has been unchanged. In the case of 3000Hz switching losses has a magnitude of 20 and conduction loss has a magnitude of 10. The resultant losses is therefore 30.The difference between switching loss and conduction loss is 10 and switching loss is greater than conduction loss. The variation of the switching loss from the previous case is due to the increase in frequency. The magnitude of the conduction losses remains constant as the duty cycle has been unchanged.

5.2. For the switch Sa4

In the case of 1000Hz switching losses is almost equivalent to 0 and conduction loss has a magnitude more than 25. The resultant losses is therefore 30. The difference between conduction loss and switching loss is 28 and conduction loss is greater than switching loss. There is a small difference between the conduction losses and total losses. In the case of 2000Hz switching losses is almost equivalent to 0 and conduction loss has a magnitude of 30. The resultant losses are therefore 30. The difference between conduction loss and switching loss is 30 and conduction loss is greater than switching loss. There is no difference, and the peaks perfectly coincide between the conduction losses and total losses. In the case of 5000Hz switching losses is almost equivalent to 5 and conduction loss has a magnitude of 25. The resultant losses is therefore 30. The difference between conduction loss and switching loss is 25 and conduction loss is greater than switching loss. There is a slight difference between the conduction losses and total losses thus it brings us to the conclusion that conduction losses are dominating over switching losses over the change in frequency.

The simulation is done in two cases. In case 1, Switching frequency is varied in steps of 1000 Hz ,2000 Hz and 5000 Hz and the reference frequency is set to constant hence the speed.

For 1000 Hz, ψ_d and ψ_q represent the machine flux. In PMSM the ψ_q is equivalent to 0. So initially it may have some value but gradually it ceases to exist. Due to the change in frequency the electromagnetic torque changes from 8.2 to 11.5 N-m. There is an increase of 3.3 N-m of torque for changing the switching frequency to 1000Hz.Speed in rpm is constant. For 2000 Hz, ψ_d and ψ_q represent the machine flux. In PMSM the ψ_q is equivalent to 0. So initially it may have some value but gradually it ceases to exist. Due to the change in frequency the electromagnetic torque changes from 9 to 10.8 N-m. There is an increase of 1.8 N-m of torque for changing the switching frequency to 2000Hz.Speed in rpm is constant. For 3000 Hz, ψ_d and ψ_q represent the machine flux. In PMSM the ψ_q is equivalent to 0. So initially it may have some value but gradually it ceases to exist. Due to the change in frequency the electromagnetic torque changes from 9.6 to 10.3 N-m. There is an increase of 0.7 N-m of torque for changing the switching frequency to 3000Hz.Speed in rpm is constant. In all the three cases as the switching frequency increase the difference between torques decrease while the speed remains constant.

In case 2, Switching frequency is kept constant at 1000Hz and the reference sine frequency is varied in steps of 10Hz, 30Hz, 50Hz and 70Hz

For 10Hz, ψ_d and ψ_q represent the machine flux. ψ_d increases from 1.027 to 1.047. ψ_q is slightly increased from 0.075 to 0.085. The electromagnetic torque changes from 9 to 11N-m. There is an increase of 2 N-m of torque. For 30Hz, ψ_d and ψ_q represent the machine flux. ψ_d increases from 0.87 to 0.917. ψ_q is slightly increased from 0.085 to 0.08. The electromagnetic torque changes from 8.8 to 11.2N-m. There is an increase of 2.4 N-m of torque. For 50Hz, ψ_d and ψ_q represent the machine flux. ψ_d increases from 0.727 to 0.758. ψ_q is slightly increased from 0.07 to 0.095. The electromagnetic torque changes from 8 to 11.5N-m. There is an increase of 3.5 N-m of torque. The quadrature axis flux component remains same and equal to zero.

6. Conclusion

The paper provides the torque ripples and switching losses data. It is observed that the switching losses are considerably high in Sa1 compared to Sa4. As the switching frequency is increased, the switching losses dominates conduction losses. At 1000 Hz, the switching loss and conduction losses are approximately equal. It is observed that the torque ripple is around 5 N-m for 5000 Hz switching frequency. As the speed of the PMSM increased, The direct axis flux component is proportionally decreases and the torque remains unchanged as the load torque is kept constant at 10 N-m.

Compliance with ethical standards

Acknowledgments

We appreciate the management of CVR College of Engineering for providing the lab facilities in getting the results of this work in time.

Disclosure of conflict of interest

The authors declare no conflict of interests.

References

[1] Noriya Nakao, Kan Akatsu. Suppressing pulsating torques: torque ripple control of synchronous motors, IEEE Industry Applications Magazine. Nov-Dec 2014; 20(6).

[2] Hai Shang, Linhui Zhao, Tong Wang. Torque ripple reduction for permanent magnet synchronous motor based on learning control", 2015 2nd International conference on information science and control engineering. April 2015; 15201908: 24-26.

[3] Chen Li, Changliang Xia, Zhanqing Zhou, Tingna Shi Yan Yan. Torque ripple reduction for permanent magnet synchronous motor based on predictive sequence control. 2017 20th International Conference on Electrical Machines and Systems (ICEMS), 11-14 August 2017.

[4] Lang Bao-hua, Liu Wei-guo, Zhou Xi-wei, Li Rong. Research on Direct Torque Control of Permanent Magnet Synchronous Motor Based on Optimized State Selector", 2006 IEEE International Symposium on Industrial Electronics. july 2006; 9-13.

[5] Cong Xiong, Haiping Xu, Cheng Fang, Haiyang Zhang. Direct Torque Control of Permanent-Magnet Synchronous Machine Drives With Reduced Torque Ripple and Strong Robustness, 2017 IEEE Transportation Electrification Conference and Expo, Asia-Pacific (ITEC Asia-Pacific), 07-10 August 2017.

[6] Yuchi Feng, Haiyan Zhao, Mingxing Zhao, Hong Chen. A feedbackLinearization control scheme based on direct torque control for permanent magnet synchronous motor", 2018 37th Chinese Control Conference (CCC). July 2018; 25-27.

[7] Mathworks.com – Loss Calculation in a 3-Phase 3-Level Inverter Using SimPowerSystems and Simscape. http\\abb.com. IGBT Module 5SNE 0800M170100